

Stable and Controllable Neural Texture Synthesis and Style Transfer Using Histogram Losses

Pierre Wilmot¹, Eric Risser¹, Connelly Barnes^{1,2}

¹Artomatix, ²University of Virginia

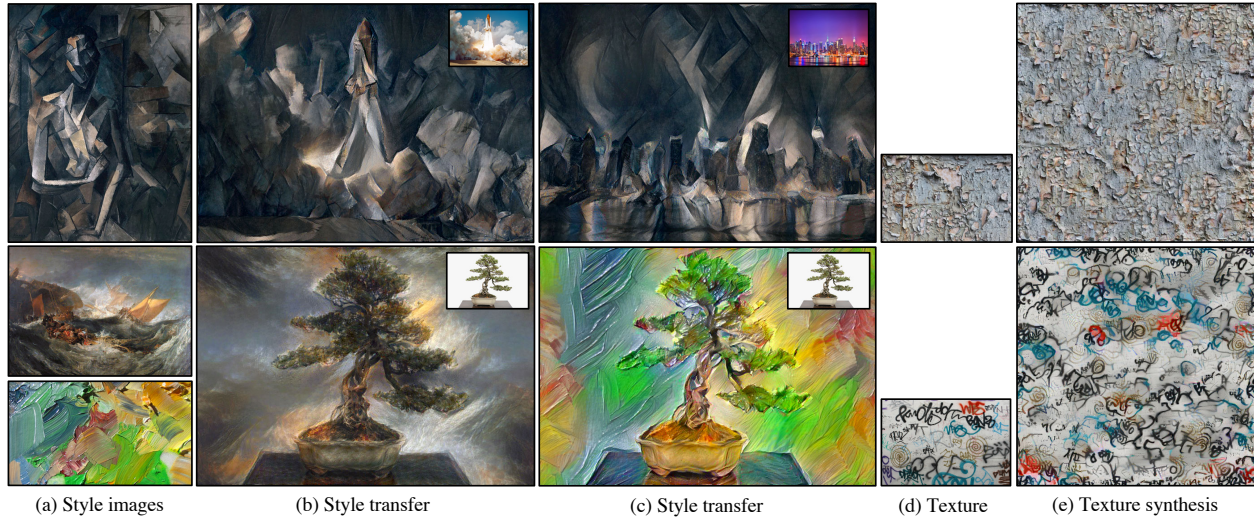


Figure 1: Our style transfer and texture synthesis results. The input styles are shown in (a), and style transfer results are in (b, c). Note that the angular shapes of the Picasso painting are successfully transferred on the top row, and that the more subtle brush strokes are transferred on the bottom row. The original content images are inset in the upper right corner. Unless otherwise noted, our algorithm is always run with default parameters (we do not manually tune parameters). Input textures are shown in (d) and texture synthesis results are in (e). For the texture synthesis, note that the algorithm synthesizes creative new patterns and connectivities in the output.

Abstract

Recently, methods have been proposed that perform texture synthesis and style transfer by using convolutional neural networks (e.g. Gatys et al. [2015; 2016]). These methods are exciting because they can in some cases create results with state-of-the-art quality. However, in this paper, we show these methods also have limitations in texture quality, stability, requisite parameter tuning, and lack of user controls. This paper presents a multiscale synthesis pipeline based on convolutional neural networks that ameliorates these issues. We first give a mathematical explanation of the source of instabilities in many previous approaches. We then improve these instabilities by using histogram losses to synthesize textures that better statistically match the exemplar. We also show how to integrate localized style losses in our multiscale framework. These losses can improve the quality of large features, improve the separation of content and style, and offer artistic controls such as paint by numbers. We demonstrate that our approach offers improved quality, convergence in fewer iterations, and more stability over the optimization.

Keywords: style transfer, texture synthesis, neural networks

Concepts: •Computing methodologies → Image manipulation; Computational photography;

Permission to make digital or hard copies of all or part of this work for personal or classroom use is granted without fee provided that copies are not made or distributed for profit or commercial advantage and that copies bear this notice and the full citation on the first page. Copyrights for components of this work owned by others than ACM must be honored. Abstracting with credit is permitted. To copy otherwise, or republish, to post on servers or to redistribute to lists, requires prior specific permission and/or a fee. Request

1 Introduction

In recent years, deep convolutional neural networks have demonstrated dramatic improvements in performance for computer vision tasks such as object classification, detection, and segmentation [Krizhevsky et al. 2012; He et al. 2016]. Because of the success of these models, there has also been much interest in adapting these architectures for synthesis tasks in graphics and computational photography. For instance, in computational photography, deep architectures have been used for many tasks, including editing of photos [Tsai et al. 2016; Yan et al. 2016; Chang et al. 2016], objects [Zhu et al. 2016], image style transfer [Gatys et al. 2016], texture synthesis [Gatys et al. 2015], new view synthesis [Kalantari et al. 2016], and image inpainting [Pathak et al. 2016; Yang et al. 2016].

In this paper, we specifically focus on the use of convolutional neural networks (CNNs) for style transfer and texture synthesis. Recently, Gatys et al. [Gatys et al. 2015; Gatys et al. 2016] proposed parametric synthesis models for these problems, which utilize CNNs. For some inputs, particularly for style transfer, these models can result in quite successful, state-of-the-art results (see Figures 9-12). However, we found as we investigated these methods in depth that they are subject to a number of limitations. These include limitations in stability, ghosting artifacts, the need for per-image parameter tuning, and challenges in reproducing large-scale features. Furthermore, these methods do not incorporate artistic controls such as painting by numbers [Hertzmann et al. 2001; Ritter et al. 2006; Lukáč et al. 2013; Lukáč et al. 2015].

permissions from permissions@acm.org. © 2017 ACM.
CONFERENCE PROGRAM NAME, MONTH, DAY, and YEAR
ISBN: THIS-IS-A-SAMPLE-ISBN...\$15.00
DOI: http://doi.acm.org/THIS/IS/A/SAMPLE/DOI

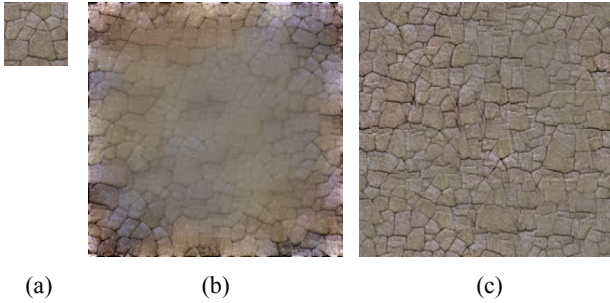


Figure 2: *Instabilities in texture synthesis of Gatys et al. [Gatys et al. 2015]. We show the input texture (a). A larger texture (b) is synthesized and shows a significant amount of instability where the brightness and contrast vary significantly throughout the image. By hand-tuning parameters, we can find parameter settings that produce pleasing results for this example (c). However, we still observe artifacts such as ghosting due to a smaller degree of instability.*

Our first contribution in this paper is a demonstration of how and why such instabilities occur in the neural network synthesis approaches (see Section 4.2). Examples of instabilities are shown in Figure 2. In neural network synthesis methods such as Gatys et al [2015; 2016], we have found that carefully tuning parameters on a per-image basis is often necessary to obtain good quality results, the optimization is often unstable over its iterations, and the synthesis process becomes more unstable as the size of the output increases.

We next demonstrate in Section 4.3 that such instabilities can be addressed by the use of novel histogram loss terms. These loss terms match not only the mean but also the statistical distribution of activations within CNN layers. We also show how to effectively minimize such histogram losses. Our histogram losses improve quality, reduce ghosting, and accelerate convergence. We initially formulate the histogram losses for texture synthesis and then in Section 4.4 discuss how to extend them for style transfer.

We next demonstrate in Section 5 how quality and control can be further improved by using localized losses in a multiscale synthesis framework. In Section 5.2, we demonstrate how localized style losses can be used to incorporate artistic controls such as paint by numbers, as well as improve separation of content and style, and better reproduce large features. In Section 6, we explain how we automatically select parameters, which removes the requirement for a human to manually tune parameters.

These contributions together allow us to achieve state-of-the-art quality for neural style transfer and for parametric neural texture synthesis.¹

2 Related work

Parametric texture synthesis. Some early methods for texture synthesis explored parametric models. Heeger and Bergen [1995] used histogram matching combined with Laplacian and steerable pyramids to synthesize textures. We are inspired by their use of histogram matching. Portilla and Simoncelli [2000] investigated the integration of many wavelet statistics over different locations, orientations, and scales into a sophisticated parametric texture syn-

¹Except for on regular textures, where Berger et al. [2016] have recently demonstrated a loss that improves regularity, which we do not currently include.

thesis method. These included cross-correlations between pairs of filter responses.

Neural texture synthesis and style transfer. In this paper, for short, we use “neural” to refer to convolutional neural networks. Recently, Gatys et al. [2015] showed that texture synthesis can be performed by using ImageNet-pretrained convolutional neural networks such as VGG [Simonyan and Zisserman 2014]. Specifically, Gatys et al. [2015] impose losses on co-occurrence statistics for pairs of features. These statistics are computed via Gram matrices, which measure inner products between all pairs of feature maps within the same layers of the CNN. The texture synthesis results of Gatys et al. [2015] typically improve upon those of Portilla and Simoncelli [2000]. Gatys et al. [2016] later extended this approach to style transfer, by incorporating within CNN layers both a Frobenius norm “content loss” to a content exemplar image, and a Gram matrix “style loss” to a style exemplar image. We build upon this framework, and offer a brief review of how it works in the next section. Concurrently to our research, Berger et al. [2016] observed that in the approach of Gatys et al., texture regularity may be lost during synthesis, and proposed a loss that improves regularity based on co-occurrence statistics between translations of the feature maps. Recently, Aittala et al. [2016] used neural networks to extract SVBRDF material models from a single photo of a texture. Their method focuses on a more specific problem of recovering a SVBRDF model from a head-lit flash image. However, they do observe that certain instabilities such as non-stationary textures can easily result if sufficiently informative statistics are not used. We see this as connected with our observations about instabilities and how to repair them.

Feedforward neural texture synthesis. Recently, a few papers [Ulyanov et al. 2016a; Ulyanov et al. 2016b; Johnson et al. 2016] have investigated the training of feedforward synthesis models, which can be pre-trained on a given exemplar texture or style, and then used to quickly synthesize a result using fixed network weights. The feed-forward strategy is faster at run-time and uses less memory. However, feed-forward methods must be trained specifically on a given style or texture, making the approach impractical for applications where such a pre-training would take too long (pre-training times of 2 to 4 hours are reported in these papers).

Non-parametric texture synthesis. Non-parametric texture synthesis methods work by copying neighborhoods or patches from an exemplar texture to a synthesized image according to a local similarity term [Efros and Leung 1999; Wei and Levoy 2000; Lefebvre and Hoppe 2005; Lefebvre and Hoppe 2006; Kwatra et al. 2003; Kwatra et al. 2005; Barnes et al. 2009]. This approach has also been used to transfer style [Efros and Freeman 2001; Hertzmann et al. 2001; Barnes et al. 2015]. Some papers have recently combined parametric neural network models with non-parametric patch-based models [Chen and Schmidt 2016; Li and Wand 2016].

3 A brief introduction to neural texture synthesis and style transfer

In this section, we briefly introduce the texture synthesis and style transfer methods of Gatys et al. [2015; 2016]. For a more thorough introduction to these techniques, please refer to those papers. We show some example results from these methods later in the paper: neural texture synthesis is shown in Figure 8, and style transfer results are shown in Figures 9-12.

For texture synthesis [Gatys et al. 2015], we are given an input source texture S , and wish to synthesize an output texture O . We pass S and O through a CNN such as VGG [Simonyan and Zisserman 2014]. This results in feature maps for the activations of

the first L convolutional layers, which we denote as $S_1 \dots S_L$ and $O_1 \dots O_L$. Then we minimize a loss $\mathcal{L}_{\text{gram}}$ over the layers, which preserves some properties of the input texture by means of a Gram matrix:

$$\mathcal{L}_{\text{gram}} = \sum_{l=1}^L \frac{\alpha_l}{|S_l|^2} \|G(S_l) - G(O_l)\|_F^2 \quad (1)$$

Here α_l are user parameters that weight terms in the loss, $|\cdot|$ is the number of elements in a tensor, $\|\cdot\|_F$ is the Frobenius norm, and the Gram matrix $G(F)$ is defined over any feature map F as an $N_l \times N_l$ matrix of inner products between pairs of features:

$$G_{ij}(F) = \sum_k F_{ik} F_{jk} \quad (2)$$

Here F_{ij} refers to feature i 's pixel j within the feature map. The synthesized output image O is initialized with white noise and is then optimized by applying gradient descent to equation (1). Specifically, the gradient of equation (1) with respect to the output image O is computed via backpropagation.

Style transfer [Gatys et al. 2016] works similarly, but we are given a content image C , style image S , and would like to synthesize a stylized output image O . We pass all three images through a CNN such as VGG, which gives activations for the first L convolutional layers of $C_1 \dots C_L$, $S_1 \dots S_L$, $O_1 \dots O_L$. Then the total style transfer loss combines the losses for the style image ($\mathcal{L}_{\text{gram}}$) and the content image:

$$\mathcal{L}_{\text{transfer}} = \mathcal{L}_{\text{gram}} + \mathcal{L}_{\text{content}} \quad (3)$$

The content loss is a feature distance between content and output, which aims to make output and content look similar:

$$\mathcal{L}_{\text{content}} = \sum_{l=1}^L \frac{\beta_l}{|C_l|} \|C_l - O_l\|_F^2 \quad (4)$$

Again, β_l are user weight parameters, and the output image O is initialized with white noise and optimized using gradient descent.

4 Our basic method using histogram losses

In this section, we present our baseline texture synthesis and style transfer method, which incorporates histogram losses. We first briefly discuss in Section 4.1 some statistics that can be useful for parametric neural network synthesis. We then demonstrate in Section 4.2 how and why instabilities occur in the previous approach of Gatys et al [2015; 2016]. We next explain in Section 4.3 how we address these instabilities using histogram losses, and how to effectively minimize histogram losses.

4.1 Prelude: useful statistics for parametric synthesis

If one revisits earlier parametric texture synthesis research such as Portilla and Simoncelli [2000], one will quickly note that many different statistics can be used for texture synthesis. We investigated the effect of matching several such statistics for neural networks in Figure 3. We show the results of matching only the mean activations of each feature (with an L^2 loss), matching Gram matrices using equation (1), the full histogram matching that we develop later in Section 4.3, and the combination of Gram matrices and our full histogram matching. Results with Gram matrix statistics tend to be generally better than results using mean activations. Results with histogram statistics are often more stable in terms of image intensity, but can break some small structures. The best results are obtained using our full method (Gram + histogram). Of course,

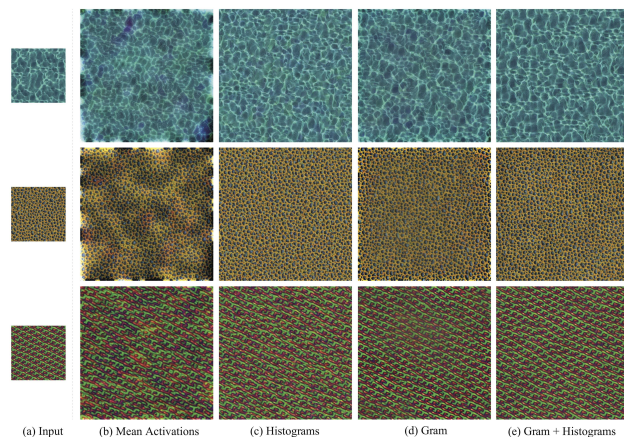


Figure 3: Different statistics that can be used for neural network texture synthesis. See the body of Section 4.1 for discussion.

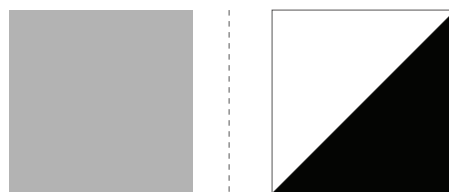


Figure 4: At left, an example input image, which has a uniform distribution of intensities with a mean of $\mu_1 = 1/\sqrt{2} \approx 0.707$ and a standard deviation of $\sigma_1 = 0$. At right, an example output image, which has a non-uniform distribution with a mean of $\mu_2 = 1/2$ and a standard deviation of $\sigma_2 = 1/2$. If interpreted as the activation of a feature map with one feature, these two distributions have equivalent non-central second moments of $1/2$, and equal Gram matrices.

additional statistics could also be investigated, such as the translational co-occurrence statistics of Berger et al. [Berger and Memisevic 2016], but this is beyond the scope of our paper.

We find it interesting that although Gram matrices are widely used for synthesis [Gatys et al. 2015; Gatys et al. 2016; Selim et al. 2016; Berger and Memisevic 2016; Johnson et al. 2016], their results are often unstable. We investigate the causes of this instability in the next section.

4.2 The problem: instabilities

The instabilities are shown in Figure 2. The cause of these is quite simple to understand. To simplify and illustrate the problem, imagine that our input image is grey, as shown in Figure 4 on the left. Our desired output from texture synthesis is thus also a grey image, with a mean value being $1/\sqrt{2}$ (about 70.7% gray). The problem is that there are many distributions that will result in an equivalent Gram matrix, such as the output image on the right of Figure 4, where half of the image is 0 (black) and the other half is 1 (white). Of course, in reality, the Gram matrices do not match image intensities, but rather *feature activations*, i.e. feature maps after applying the activation functions. However, the same argument applies: if we interpret the images of Figure 4 as feature map activations, then activation maps with quite different means and variances can still have the same Gram matrix.

It is slightly technical to understand this issue more formally. This

is because the Gram matrix is statistically related to neither the mean nor covariance matrices, but instead to the matrix of non-central second moments. We now explain this formally. Let us consider the case of a feature activation map F with m features. In the rest of this section, for brevity, we will refer to “feature map activations” simply as “features,” so all “feature” always refers to the result of applying the activation function. We can summarize the statistics of the features in the feature map F by using an m dimensional random variable \mathbf{X} to model the probability distribution of a given m -tuple of features. We can relate the random vector of features \mathbf{X} and the feature map F . For example, if we normalize the Gram matrix $G(F)$ by the number of samples n , we obtain a sample estimator for the second non-central mixed moments $E[\mathbf{X}\mathbf{X}^T]$. Consequently, in the following discussion, we will sometimes informally refer to the (normalized) “Gram matrix” and $E[\mathbf{X}\mathbf{X}^T]$ interchangeably, even though one is actually a sampled estimator for the other. For the following argument we thus set $\frac{1}{n}G(F) = E[\mathbf{X}\mathbf{X}^T]$. Define the mean feature $\boldsymbol{\mu} = E[\mathbf{X}]$. By a general property of covariance matrices, we have that $\Sigma(\mathbf{X}) = E[\mathbf{X}\mathbf{X}^T] - \boldsymbol{\mu}\boldsymbol{\mu}^T$, where Σ indicates a covariance matrix. After rearranging, we obtain:

$$E[\mathbf{X}\mathbf{X}^T] = \Sigma(\mathbf{X}) + \boldsymbol{\mu}\boldsymbol{\mu}^T \quad (5)$$

For simplicity, let us now consider the case where we have only one feature, $m = 1$. By substituting into equation (5), we obtain:

$$\frac{1}{n}G(F) = E[X^2] = \sigma^2 + \mu^2 = \|(\sigma, \mu)\|^2 \quad (6)$$

Here σ is the standard deviation of our feature X . Suppose we have a feature map F_1 for the input source image, and a feature map F_2 for the synthesized output, and that these have respective feature distributions X_1, X_2 , means μ_1, μ_2 , and standard deviations σ_1, σ_2 . Thus, from equation (6), we know that the maps will have the same Gram matrix if this condition holds:

$$\|(\sigma_1, \mu_1)\| = \|(\sigma_2, \mu_2)\| \quad (7)$$

We can easily use this to generate an infinite number of 1D feature maps with different variances but equal Gram matrix. Clearly this is bad for synthesis. Specifically, this means that even if we hold the Gram matrix constant, then *the variance σ_2^2 of the synthesized texture map can be freely change* (with corresponding changes to the mean μ_2 based on equation (7)), or conversely, that *the mean μ_2 of the synthesized texture map can freely change* (with corresponding changes to the variance, σ_2^2). This property leads to the instabilities shown in Figure 2. For simplicity, we assume that the CNN is flexible enough to generate any distribution of output image features that we request. Suppose we wish to generate an output texture with a different variance (e.g. $\sigma_2 \gg \sigma_1$) but equal Gram matrix. Then we can simply solve equation (6) for μ_2 , and obtain $\mu_2 = \sqrt{\sigma_1^2 + \mu_1^2 - \sigma_2^2}$. In fact, this is how we generated the different distributions with equal Gram matrices in Figure 4. The left distribution X_1 has $\mu_1 = 1/\sqrt{2}$ and $\sigma_1 = 0$, and we set a larger standard deviation $\sigma_2 = 1/2$ for the right distribution, so we obtain $\mu_2 = 1/2$.

In the multidimensional case $m > 1$, if there is no correlation between features, then we simply have m separate cases of the previous 1D scenario. Thus, while maintaining the same Gram matrix, we can clearly change all of the variances however we like, as long as we make a corresponding change to the mean. This can clearly lead to instabilities in variance or mean.

However, in the multidimensional scenario, typically there are correlations between features. Consider the scenario where we are given an input feature map F_1 , and thus the input feature random vector \mathbf{X}_1 and its mean $\boldsymbol{\mu}$ and covariance matrix $\Sigma(\mathbf{X}_1)$. Now,

we wish to explore the set of output feature random vectors \mathbf{X}_2 with equal Gram matrix but different variance. In computer graphics, color adjustment models based on affine operations are often explored for finding correspondences [HaCohen et al. 2011], and adjusting colors [Siddiqui and Bouman 2008], including for texture synthesis [Darabi et al. 2012; Diamanti et al. 2015]. Due to these affine models, we thought it appropriate to investigate whether synthesized textures will be stable if we hold their Gram matrix constant but otherwise allow features to undergo affine changes. We thus explored applying an affine transformation to our random vector of input feature activations \mathbf{X}_1 to obtain a transformed random vector of output feature activations $\mathbf{X}_2 = \mathbf{A}\mathbf{X}_1 + \mathbf{b}$, where \mathbf{A} is an $m \times m$ matrix, and \mathbf{b} is an m vector. Then, using equation (5), we can set the Gram matrices of \mathbf{X}_1 and \mathbf{X}_2 equal to obtain:

$$\begin{aligned} E[\mathbf{X}_2\mathbf{X}_2^T] &= \mathbf{A}\Sigma(\mathbf{X}_1)\mathbf{A}^T + (\mathbf{A}\boldsymbol{\mu} + \mathbf{b})(\mathbf{A}\boldsymbol{\mu} + \mathbf{b})^T = \\ E[\mathbf{X}_1\mathbf{X}_1^T] &= \Sigma(\mathbf{X}_1) + \boldsymbol{\mu}\boldsymbol{\mu}^T. \end{aligned} \quad (8)$$

We decided to constrain the variances of the output random feature activation vector \mathbf{X}_2 along the main diagonal of its covariance matrix, so that the variances are equal to a set of “target” output image feature activation variances. We can then solve for the remaining unknown variables in the transformation matrix \mathbf{A} and vector \mathbf{b} . Unfortunately, closed-form solutions of the resulting quadratic equations appear to generate multi-page long formulas, even for the two-dimensional case. However, intuitively, there are more unknowns than equations, so it should often be possible to generate a output feature distribution \mathbf{X}_2 with different variances than the input texture’s feature distribution \mathbf{X}_1 , but with the same Gram matrix. Specifically, there are $m(m+1)$ unknowns for \mathbf{A} and \mathbf{b} , whereas there are only $m(m+3)/2$ constraints, due to equation (8) ($m(m+1)/2$ constraints due to the upper half of the symmetric matrix, plus m constraints for the known output feature variances).

To verify the intuition that it is possible to construct multidimensional distributions that are related by affine transformations and have different variance but equal Gram matrices, we ran extensive numerical experiments for solving the equations 8 in dimensions $m = 1 \dots 16, 32, 64$. We found that in every case there was a solution. Specifically, we generated large numbers of mean and covariance matrices for the feature distributions of the input texture, and the output feature variances, with each sampled from the uniform distribution $U(0, 1)$.

We conclude that there are many ways to change the variance of an input texture without changing its Gram matrix. This leads to the instabilities shown in Figure 2.

We also note that recent papers on neural texture synthesis (e.g. [Gatys et al. 2015; Ulyanov et al. 2016a; Berger and Memisevic 2016]) usually demonstrate outputs at the same resolution or slightly larger than the input. This is a departure from papers in computer graphics, which traditionally synthesized output texture at a significantly larger size than the input exemplar [Efros and Leung 1999; Wei and Levoy 2000; Lefebvre and Hoppe 2005; Lefebvre and Hoppe 2006; Kwatra et al. 2003; Kwatra et al. 2005]. For smaller texture sizes, the instability artifact is more subtle and can be partially mitigated by manually tweaking learning rates and gradient sizes and which layers in the network contribute to the optimization process (but it can still be observed in results, e.g. [Gatys et al. 2015; Berger and Memisevic 2016]). The instability artifact grows as the output texture is enlarged.

4.3 Solution: Histogram Losses

As we have just discussed, previous neural texture synthesis models [Gatys et al. 2015; Gatys et al. 2016; Berger and Memisevic 2016]

typically use Gram matrices to guide the synthesis process. This results in instabilities due to not providing guarantees that the mean or variance of the texture is preserved. One improvement could be to explicitly preserve statistical moments of various orders in the texture’s activations. However, we took a further step and decided to just preserve the entire histogram of the feature activations. More specifically, we augment the synthesis loss with m additional histogram losses, one for each feature in each feature map. These can be viewed as matching the marginal distributions of each feature’s activations. We also incorporate a total variation loss [Johnson et al. 2016], which improves smoothness slightly in the output image.

Thus, our combined loss for texture synthesis is:

$$\mathcal{L}_{\text{texture}}^{(\text{ours})} = \mathcal{L}_{\text{gram}} + \mathcal{L}_{\text{histogram}} + \mathcal{L}_{\text{tv}} \quad (9)$$

However, it is slightly subtle to develop a suitable histogram loss. Suppose we take the naive approach and directly place an L^2 loss between histograms of the input source texture S and the output image O . Then this loss has zero gradient almost everywhere, so it does not contribute to the optimization process.

Instead, we propose a loss based on histogram matching. First, we transform the synthesized layerwise feature activations so that their histograms match the corresponding histograms of the input source texture S . This matching must be performed once for each histogram loss encountered during backpropagation. We then add a loss between the original activations and activations after histogram matching.

We simply use an ordinary histogram matching technique [Wikipedia 2017] to remap the synthesized output activations to match the activations of the input source texture S . Let O_{ij} be the output activations for convolutional layer i , feature j , and O'_{ij} be the remapped activations. We compute the normalized histogram for the output activations O_{ij} and match it to the normalized histogram for the activations of input source texture S , thus obtaining the remapped activations O'_{ij} . We repeat this for each feature in the feature map.

Once our output activations have been updated to mimic the input source texture, we find the Frobenius norm distance between the original activations and the remapped ones. Let O_i be the activation map of feature map i and $R(O_i)$ be the histogram remapped activation map. Then we have:

$$\mathcal{L}_{\text{histogram}} = \sum_{l=1}^L \gamma_l \|O_i - R(O_i)\|_F^2 \quad (10)$$

Here γ_l is a user weight parameter that controls the strength of the loss.

To compute the gradient of this loss for backpropagation, we observe that the histogram remapping function $R(O_i)$ has zero gradient almost everywhere, and therefore can be effectively treated as a constant for the gradient operator. Therefore, the gradient of equation (10) can be computed simply by realizing $R(O_i)$ into a temporary array O'_i and then computing the Frobenius norm loss between O_i and O'_i .

4.4 Extension to style transfer

The problem definition for style transfer can be thought of as a broadening of the texture synthesis problem. Texture synthesis is the problem of statistically resynthesizing an input texture. Style transfer is similar: one statistically resynthesizes an input style exemplar S with the constraint that we also do not want the synthesized image O to deviate too much from a content image C .

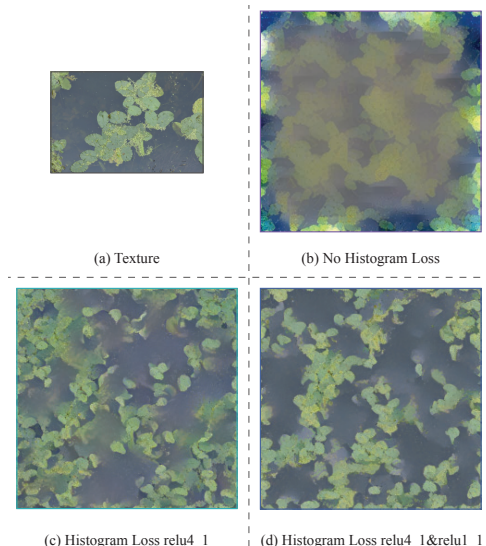


Figure 5: *Instability and ghosting: in addition to instability problems, the baseline synthesis method [Gatys et al. 2015] using Gram matrices tends to interpolate sharp transitions in colors. As we discuss in Section 7, our implementation uses the VGG-19 network [Simonyan and Zisserman 2014]. If we add a histogram loss (equation (10)) at later convolutional layers (rectified linear unit or “relu” 4_1 in VGG-19), this solves the instability issue, but the large overlapping receptive fields tend to blend features and create gradients where none exist in the input. If we also add a histogram loss to the first layer (relu 1_1), this ameliorates this problem.*

We have found that style transfer also suffers from the same instability artifacts we have shown in texture synthesis. Introducing histogram loss can offer the same benefits for this problem as well. Our style transfer strategy therefore follows Gatys et al. [2016]. We include both a per-pixel content loss and a histogram loss in the parametric texture synthesis equation. After including these, the overall style transfer loss becomes:

$$\mathcal{L}_{\text{transfer}}^{(\text{ours})} = \mathcal{L}_{\text{gram}} + \mathcal{L}_{\text{histogram}} + \mathcal{L}_{\text{content}} + \mathcal{L}_{\text{tv}} \quad (11)$$

5 Localized losses for control and stability

One concern with the parametric neural texture synthesis and style transfer approaches is that they do not include manual and automatic control maps that were previously used in non-parametric approaches [Hertzmann et al. 2001; Barnes et al. 2009; Diamanti et al. 2015; Fišer et al. 2016]. We first introduce our multiresolution (pyramidal) synthesis approach. Then we introduce a localized style loss for adding artistic user controls.

5.1 Multiresolution synthesis

For both texture synthesis and style transfer, we have found results are generally improved by a coarse-to-fine synthesis using image pyramids [Burt and Adelson 1983]. We use a ratio of two between successive image widths in the pyramid. We show in Figure 6 a comparison of pyramid and non-pyramid results. We use pyramids for all results in this paper unless otherwise indicated.

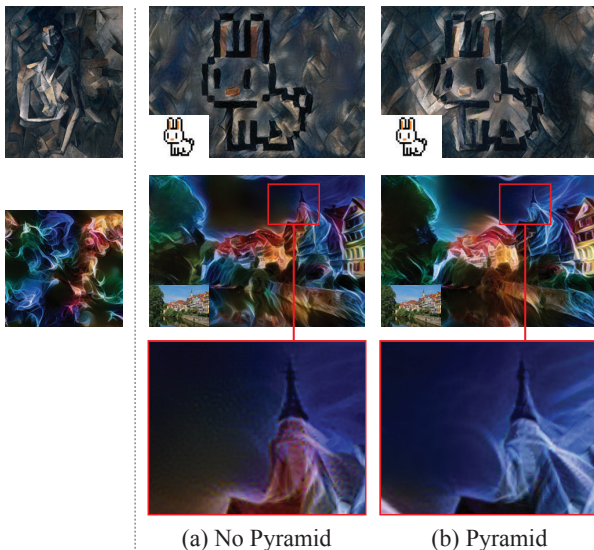


Figure 6: Comparison of pyramid and non-pyramid results. Style images are shown at left, and content images are shown inset. First row: pyramids blend coarse scale style features in with content features better. Second row: pyramids transfer coarse scale features better and reduce CNN noise artifacts. Third row: a zoom in from the second row, showing noise artifacts (at left) and better transfer of coarse-scale features (at right).

5.2 Localized style loss for artistic controls

Our approach for localizing loss functions is to make the observation that many images or styles are actually not a single texture but a collection of completely different textures laid out in a scene. As such it does not make sense to combine multiple textures into a single parametric model. Instead, we separate them out into multiple models. This approach has been known as “painting by numbers” or “painting by texture” in the literature [Hertzmann et al. 2001; Ritter et al. 2006; Lukáč et al. 2013; Lukáč et al. 2015]. This way of framing the problem has advantages for both texture synthesis and style transfer.

One way to do this would be to use multiple CNNs for different regions, and blend the regions together. However, that approach would be less efficient, and might introduce problems for the blending in transition regions. Instead, we perform painting by numbers synthesis in a single CNN.

As an input, the artist paints an “indexed mask,” where indices are painted on both the source texture (or style image) and the output image. An example of these masks is shown in Figure 7. We assume there are M indices.

Our localized style loss algorithm then proceeds by first collecting the pixels associated with each of the M indexed regions within the texture or style exemplar S . For each region, we build a different Gram matrix and list of histograms.² We track the indices also on the synthesized output O , also tracking them as necessary through an image pyramid for coarse-to-fine synthesis. During synthesis, we modify our previous losses (Equations 11 and 9) to be spatially varying. Specifically, we impose spatially varying Gram and histogram losses, where the style exemplar Gram matrices and exemplar histograms vary spatially based on the output index for the current pixel. For the histogram matching, we simply perform

²One histogram is built for each feature, the same as in Section 4.3.

the matching separately within each of the M regions defined by the indexed masks. Because the receptive fields for adjacent pixels overlap, backpropagation automatically performs blending between adjacent regions.

For style transfer it is important to note that often both the style and content images contain sets of textures that are semantically similar and should be transferred to each other. An example of this is shown in Figure 7. Using this approach we can transfer higher level style features such as eyes and lips, rather than just the lower order style features such as color and brush strokes. In Figure 7 we also show a comparison of the results of our method against Selim et al. [2016], which is a specialized method designed only for faces. For our method, we had to manually paint masks, unlike Selim et al. [2016], however, our method can apply to many domains and is not specific to faces.

6 Automatic tuning of parameters

To obtain the best results, previous methods such as Gatys et al. [2016] would often manually tune parameters on a per-image basis. With our method, of course, the same tuning of parameters could be performed manually. However, this manual tuning process can be quite tedious. Thus, for all of our results, our method automatically determines the parameters. To ensure a fair comparison with previous approaches such as Gatys et al. [2016], we also automatically determine their parameters in the figures throughout our paper, by selecting the default parameter values³. We also show in a supplemental PDF a comparison of our automatic method with hand-tuned parameters for Gatys et al. [2016]. We now describe our automatic parameter tuning process.

The parameters refer to the coefficients α_l in the Gram loss of equation (1), β_l in the content loss of equation (4), γ_l in the histogram loss of equation (10), and a fourth parameter we call ω that is multiplied against the total variation loss [Johnson et al. 2016].

Our automatic tuning process is inspired by approaches such as batch normalization [Ioffe and Szegedy 2015], which tune hyperparameters during the training process so as to prevent extreme values for gradients. We thus dynamically adjust the parameters α_l , β_l , γ_l , ω during the optimization process. Presently, our dynamic tuning is carried out with the aid of gradient information. We acknowledge that the optimization would likely be more mathematically well-founded if we instead dynamically tuned based on non-gradient information such as the magnitude of the losses or statistics within the losses. Nevertheless, this is what we currently do. During backpropagation, we encounter different loss terms \mathcal{L}_i , each of which has an associated parameter c_i that needs to be determined (c_i is one of the parameters α_l , β_l , γ_l , ω). We first calculate the backpropagated gradient \mathbf{g}_i from the current loss term as if c_i were 1. However, if the magnitude of \mathbf{g}_i exceeds a constant magnitude threshold T_i , then we normalize the gradient \mathbf{g}_i so its length is equal to T_i . We use magnitude thresholds of 1 for all parameters except for the coefficient α_l of the Gram loss, which has a magnitude threshold of 100.

7 Implementation details

This section describes our implementation in more detail. Similarly to the previous literature, we also based our implementation on the VGG-19 network, which is pre-trained on the ImageNet dataset [Simonyan and Zisserman 2014]. We use layers relu (rectified linear

³We use Johnson’s code [2015] for the comparisons with Gatys et al. [2016]

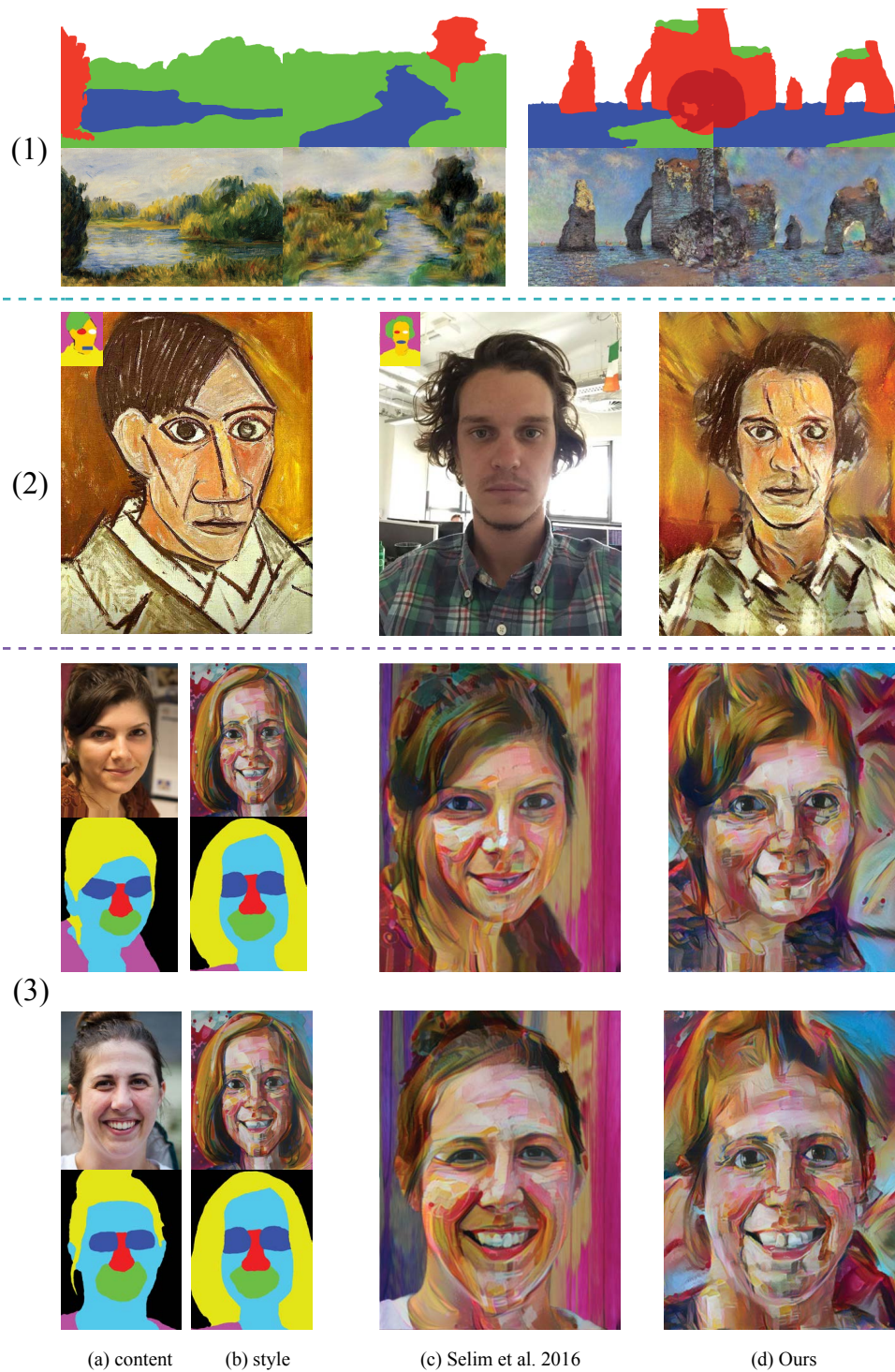


Figure 7: (1) *Painting by Numbers:* Here we show a first example of controllable parametric neural texture synthesis. Original images are on the left, synthesis results on the right, corresponding masks above each image. (2) One example of portrait style transfer using painting by numbers. (3) A second example of portrait style transfer. We show style transfer results for our method as compared to Selim et al. [2016]. Shown are the content (a) and style image (b). For our method, these need to be augmented with indexed masks, as described in Section 5.2. In (c) and (d) are the results of Selim et al. [2016] and our method. Note that our method preserves fine-scale artistic texture better. However, our method also transfers a bit more of the person’s “identity,” primarily due to hair and eye color changes. Nevertheless, our method is not specialized for faces, so this is already an interesting result.

unit) 1_1, relu 2_1, relu 3_1 and relu 4_1 for the Gram losses in texture synthesis and style transfer. The histogram losses are computed only at layers relu 4_1 and relu 1_1 (other layers are ignored: this is equivalent to fixing their weights as zero in the loss). Content loss is computed only at relu 4_1 when doing style transfer. The total variation loss smooths out noise that results from the optimization process and is thus performed only on the first convolutional layer.

As noted in Section 5.1, we synthesize our images in a multi-resolution process. We convert our input images into a pyramid. During synthesis, we start at the bottom of the pyramid, initialize to white noise, and after each level is finished synthesizing we use bi-linear interpolation to upsample to the next level.

Rather than adding a padding in our network, we instead opt for circular convolution. This produces textures that tile with themselves and does not seem to cause any strange effects during style transfer.

8 Results and discussion

Results for our texture synthesis method are shown in Figure 8. Our style transfer results are shown in Figure 9, Figure 10, Figure 11 and Figure 12. Our supplemental HTML includes many more results.

We now discuss some advantages of our result. Our histogram loss addresses instabilities by ensuring that the full statistical distribution of the features is preserved. In addition to improving image quality, our full loss (including the histogram loss) also requires fewer iterations to converge. We use a mean of 700 iterations for our results, which we find consistently give good quality, and 1000 iterations for the results of Gatys et al [2016], which we find is still sometimes unstable at that point. We note that methods based on Gram matrices such as Gatys et al [Gatys et al. 2016] can become unstable over the iteration count. We interpret this as being caused by the mean and variance being free to drift, as we discussed in Section 4.2. By adding histograms to our loss function, the result is more stable and converges better, both spatially and over iterations.

Running times for our method are as follows. We used a machine with four physical cores (Intel Core i5-6600k), with 3.5 GHz, 64 GB of RAM, and an Nvidia Geforce GTX1070 GPU with 8 GB of GPU RAM, running ArchLinux. For a single iteration on the CPU, our method takes 7 minutes and 8 seconds, whereas Gatys et al. [2016] takes 15 minutes 35 seconds. This equates to our method requiring only 45.7% of the running time for the original Gatys method. Our approach used three pyramid levels and histogram loss at relu4_1 and relu1_1. These metrics were measured over 50 iterations synthesizing a 512x512 output. We currently have most but not all of our algorithm implemented on the GPU. Because not all of it is implemented on the GPU, a speed comparison with our all-GPU implementation of Gatys et al. [2016] is not meaningful, therefore we ran both approaches using CPU only.

9 Conclusion

The key insight of this paper is that the loss function introduced by Gatys et al. [2015] and carried forward by follow-up papers can be improved in stability and quality by imposing histogram losses, which better constrain the dispersion of the texture statistics. We also show improvements by automating the parameter tuning, and in artistic controls. This paper improves on these aspects for both texture synthesis and style transfer applications.

References

AITTALA, M., AILA, T., AND LEHTINEN, J. 2016. Reflectance modeling by neural texture synthesis. *ACM Transactions on*

Graphics (TOG) 35, 4, 65.

BARNES, C., SHECHTMAN, E., FINKELSTEIN, A., AND GOLDMAN, D. 2009. Patchmatch: a randomized correspondence algorithm for structural image editing. *ACM Transactions on Graphics-TOG* 28, 3, 24.

BARNES, C., ZHANG, F.-L., LOU, L., WU, X., AND HU, S.-M. 2015. Patchtable: efficient patch queries for large datasets and applications. *ACM Transactions on Graphics (TOG)* 34, 4, 97.

BERGER, G., AND MEMISEVIC, R. 2016. Incorporating long-range consistency in cnn-based texture generation. *arXiv preprint arXiv:1606.01286*.

BURT, P., AND ADELSON, E. 1983. The laplacian pyramid as a compact image code. *IEEE Transactions on communications* 31, 4, 532–540.

CHANG, H., YU, F., WANG, J., ASHLEY, D., AND FINKELSTEIN, A. 2016. Automatic triage for a photo series. *ACM Transactions on Graphics (TOG)*.

CHEN, T. Q., AND SCHMIDT, M. 2016. Fast patch-based style transfer of arbitrary style. *arXiv preprint arXiv:1612.04337*.

DARABI, S., SHECHTMAN, E., BARNES, C., GOLDMAN, D. B., AND SEN, P. 2012. Image melding: Combining inconsistent images using patch-based synthesis. *ACM Trans. Graph.* 31, 4, 82–1.

DIAMANTI, O., BARNES, C., PARIS, S., SHECHTMAN, E., AND SORKINE-HORNUNG, O. 2015. Synthesis of complex image appearance from limited exemplars. *ACM Transactions on Graphics (TOG)* 34, 2, 22.

EFROS, A. A., AND FREEMAN, W. T. 2001. Image quilting for texture synthesis and transfer. In *Proceedings of the 28th annual conference on Computer graphics and interactive techniques*, ACM, 341–346.

EFROS, A. A., AND LEUNG, T. K. 1999. Texture synthesis by non-parametric sampling. In *Computer Vision, 1999. The Proceedings of the Seventh IEEE International Conference on*, vol. 2, IEEE, 1033–1038.

FIŠER, J., JAMRIŠKA, O., LUKÁČ, M., SHECHTMAN, E., ASENTE, P., LU, J., AND ŠŸKORA, D. 2016. Styliit: illumination-guided example-based stylization of 3d renderings. *ACM Transactions on Graphics (TOG)* 35, 4, 92.

GATYS, L., ECKER, A. S., AND BETHGE, M. 2015. Texture synthesis using convolutional neural networks. In *Advances in Neural Information Processing Systems*, 262–270.

GATYS, L. A., ECKER, A. S., AND BETHGE, M. 2016. Image style transfer using convolutional neural networks. In *Proceedings of the IEEE Conference on Computer Vision and Pattern Recognition*, 2414–2423.

HACOHEN, Y., SHECHTMAN, E., GOLDMAN, D. B., AND LISCHINSKI, D. 2011. Non-rigid dense correspondence with applications for image enhancement. *ACM transactions on graphics (TOG)* 30, 4, 70.

HE, K., ZHANG, X., REN, S., AND SUN, J. 2016. Deep residual learning for image recognition. In *2016 IEEE Conference on Computer Vision and Pattern Recognition (CVPR)*, 770–778.

HEEGER, D. J., AND BERGEN, J. R. 1995. Pyramid-based texture analysis/synthesis. In *Proceedings of the 22nd annual conference on Computer graphics and interactive techniques*, ACM, 229–238.

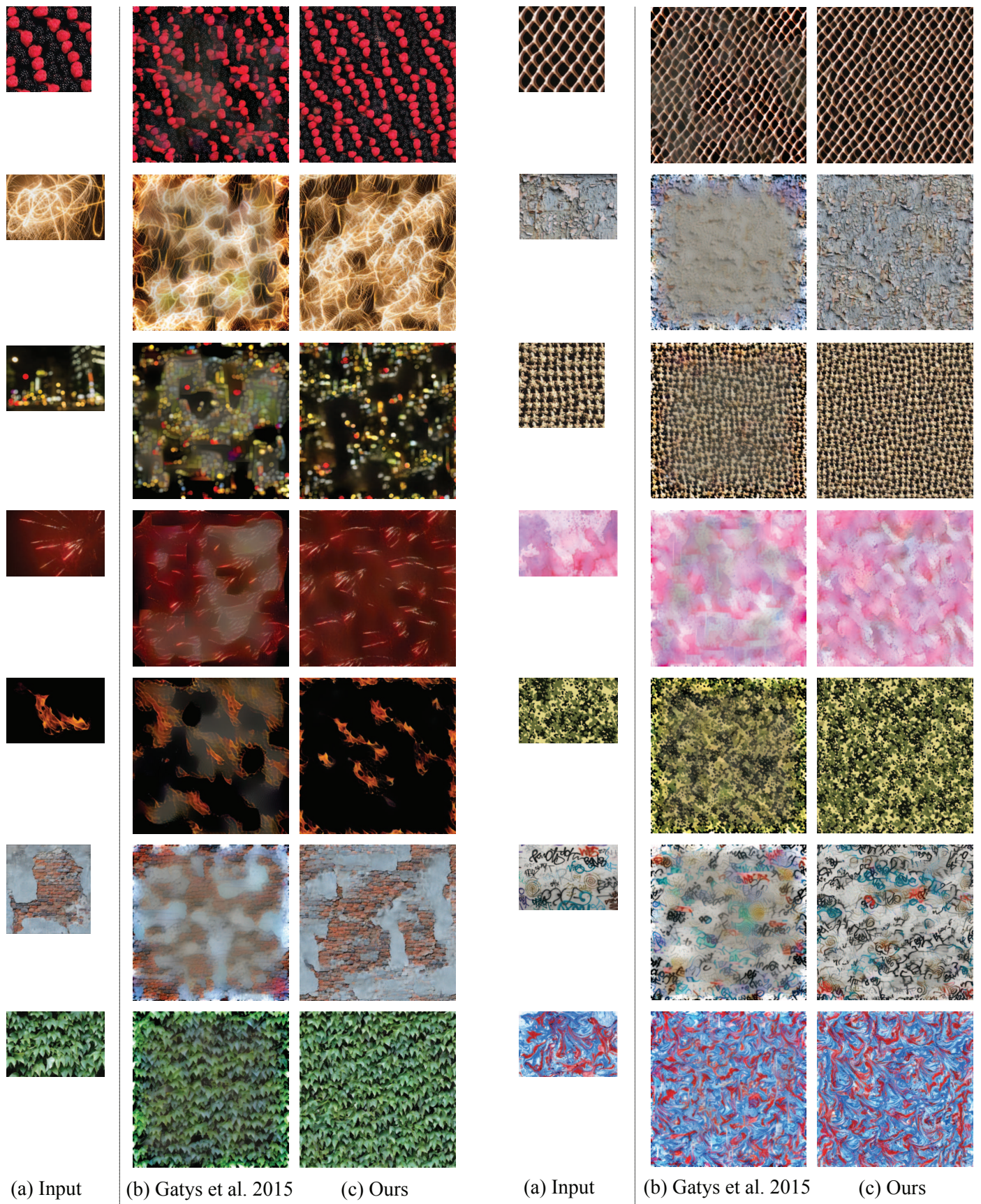


Figure 8: Results of our method for texture synthesis. Our Gatys results were generated from Johnson’s code [Johnson 2015].

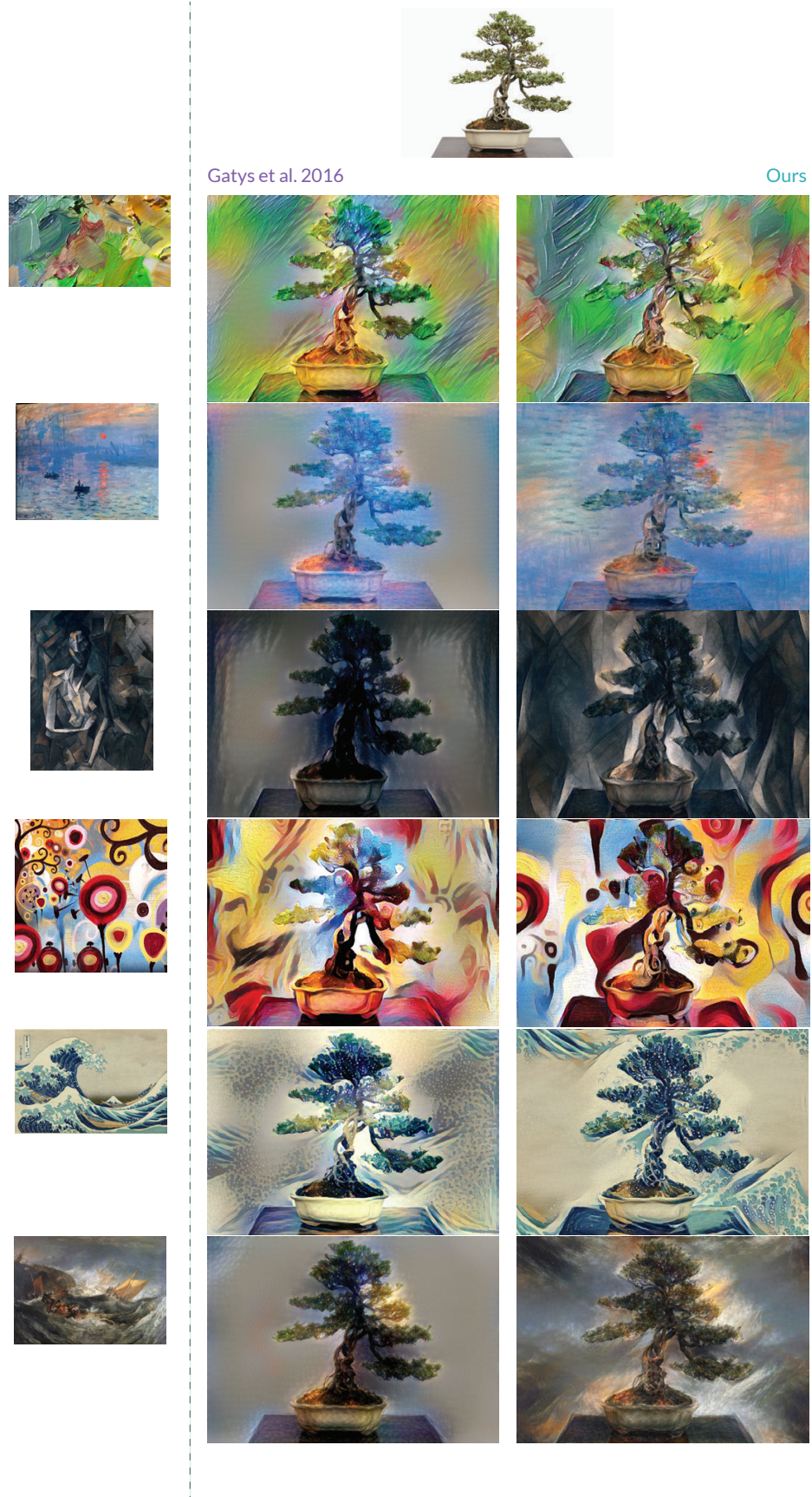


Figure 9: Results of our method for style transfer. Bonsai image from *BonsaiExperience.com*.

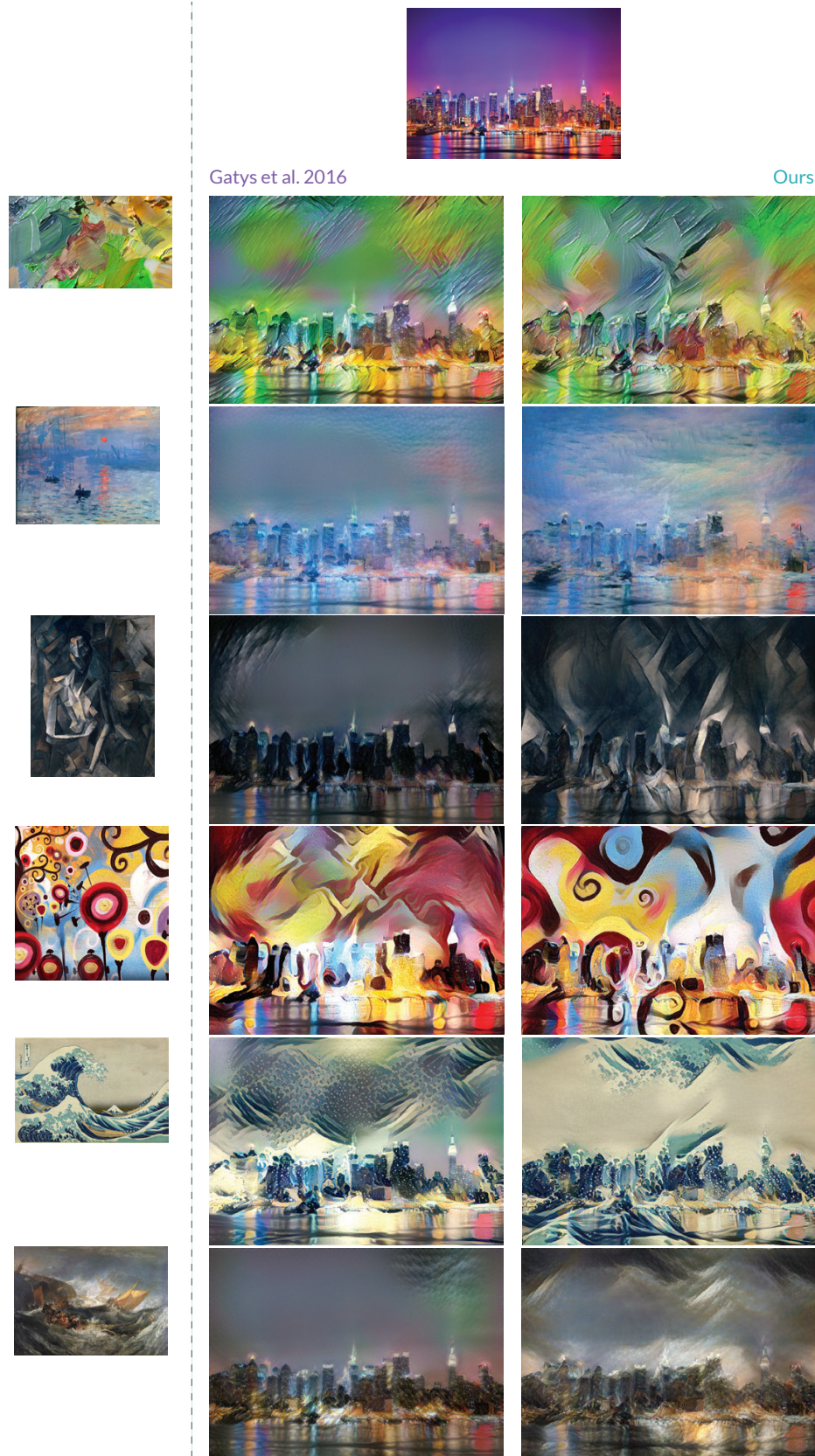


Figure 10: Results of our method for style transfer. Photo from Flickr user Wilerson S Andrade.

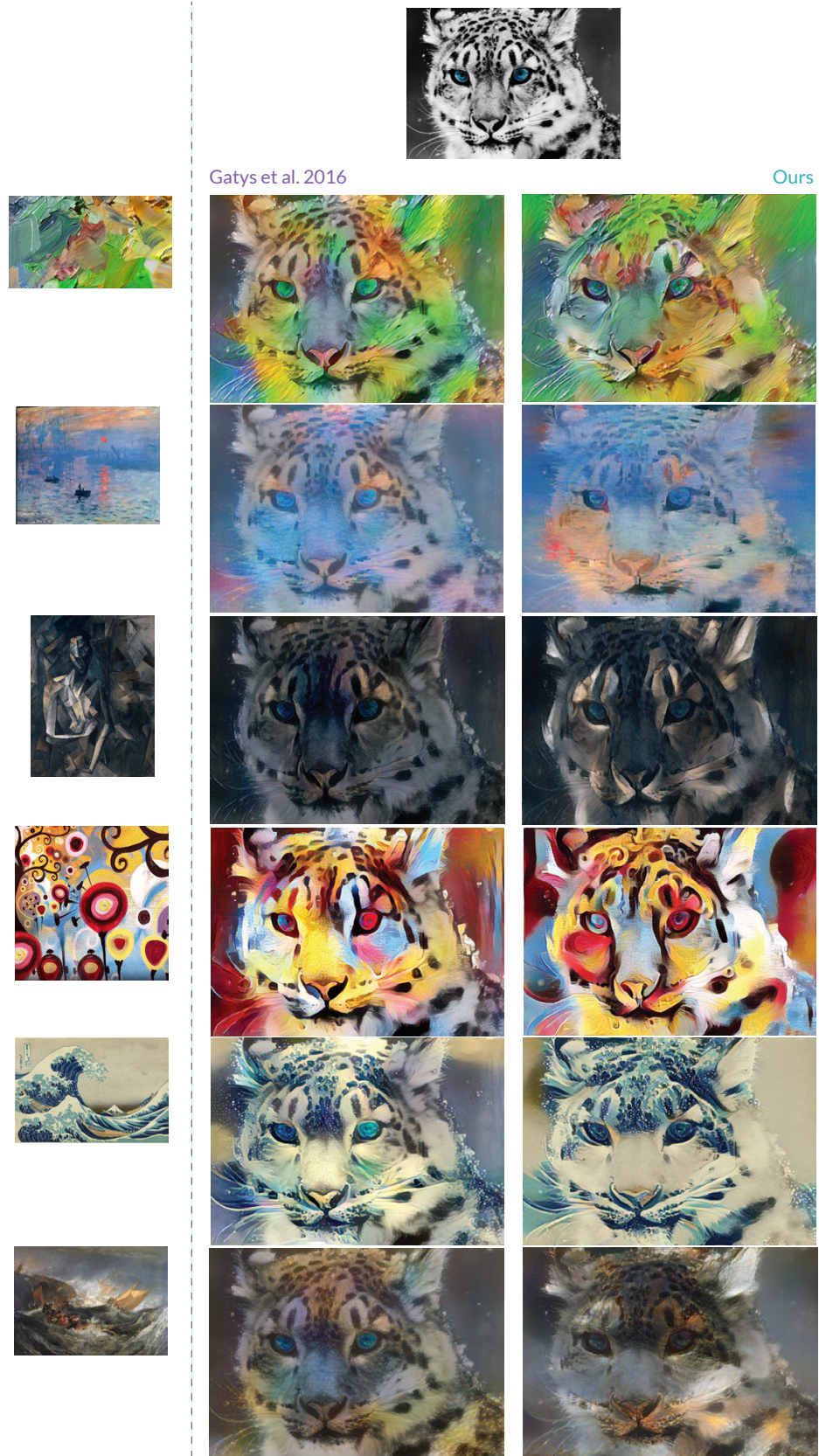


Figure 11: Results of our method for style transfer.

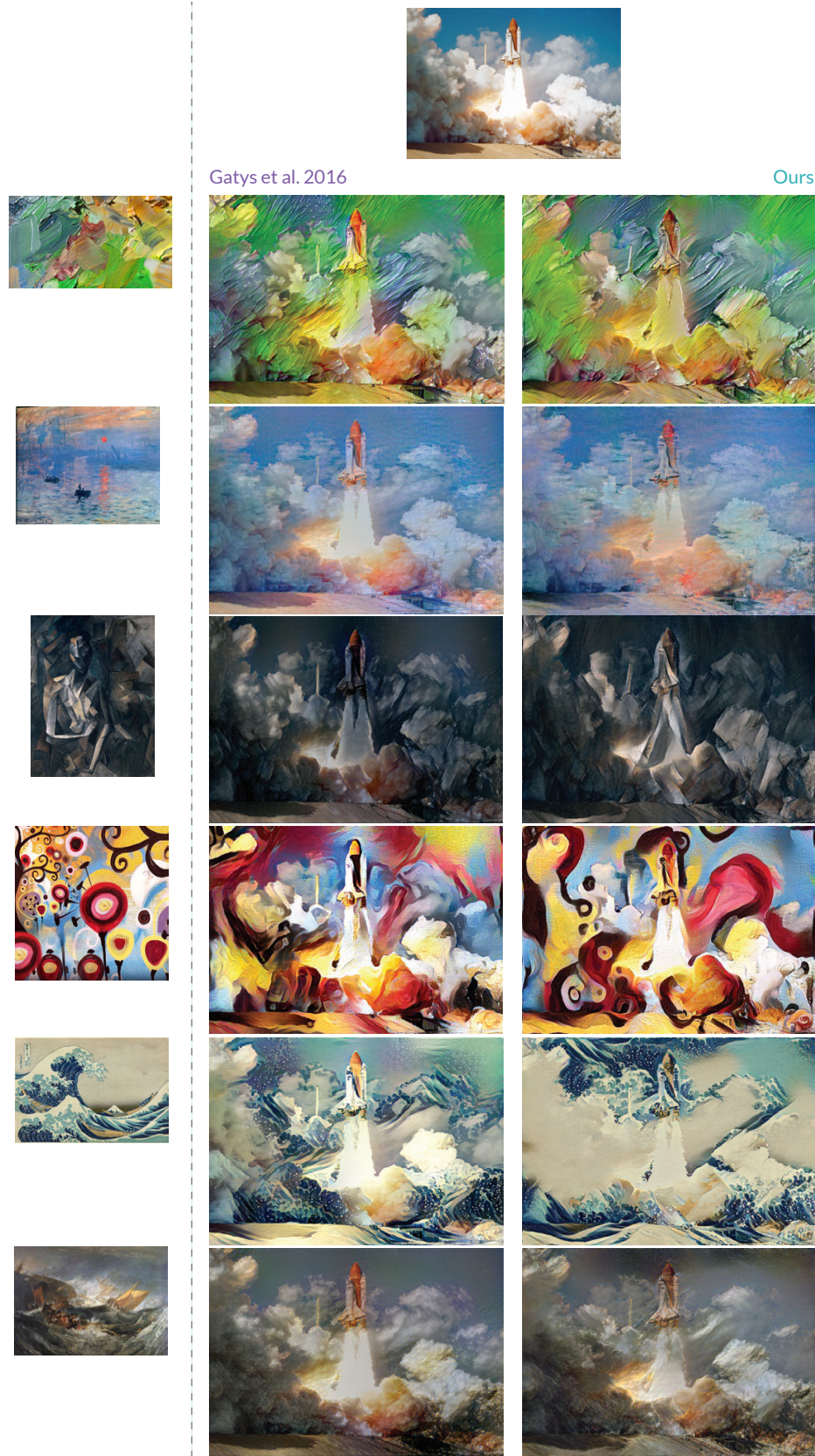


Figure 12: Results of our method for style transfer. Image from NASA.

- HERTZMANN, A., JACOBS, C. E., OLIVER, N., CURLESS, B., AND SALESIN, D. H. 2001. Image analogies. In *Proceedings of the 28th annual conference on Computer graphics and interactive techniques*, ACM, 327–340.
- IOFFE, S., AND SZEGEDY, C. 2015. Batch normalization: Accelerating deep network training by reducing internal covariate shift. *arXiv preprint arXiv:1502.03167*.
- JOHNSON, J., ALAHI, A., AND FEI-FEI, L. 2016. *Perceptual Losses for Real-Time Style Transfer and Super-Resolution*. Springer International Publishing, Cham, 694–711.
- JOHNSON, J., 2015. neural-style. <https://github.com/jcjohnson/neural-style>.
- KALANTARI, N. K., WANG, T.-C., AND RAMAMOORTHI, R. 2016. Learning-based view synthesis for light field cameras. *ACM Transactions on Graphics (TOG)* 35, 6, 193.
- KRIZHEVSKY, A., SUTSKEVER, I., AND HINTON, G. E. 2012. Imagenet classification with deep convolutional neural networks. In *Advances in neural information processing systems*, 1097–1105.
- KWATRA, V., SCHÖDL, A., ESSA, I., TURK, G., AND BOBICK, A. 2003. Graphcut textures: image and video synthesis using graph cuts. In *ACM Transactions on Graphics (ToG)*, vol. 22, ACM, 277–286.
- KWATRA, V., ESSA, I., BOBICK, A., AND KWATRA, N. 2005. Texture optimization for example-based synthesis. *ACM Transactions on Graphics (ToG)* 24, 3, 795–802.
- LEFEBVRE, S., AND HOPPE, H. 2005. Parallel controllable texture synthesis. In *ACM Transactions on Graphics (ToG)*, vol. 24, ACM, 777–786.
- LEFEBVRE, S., AND HOPPE, H. 2006. Appearance-space texture synthesis. *ACM Transactions on Graphics (TOG)* 25, 3, 541–548.
- LI, C., AND WAND, M. 2016. Combining markov random fields and convolutional neural networks for image synthesis. *arXiv preprint arXiv:1601.04589*.
- LUKÁČ, M., FIŠER, J., BAZIN, J.-C., JAMRIŠKA, O., SORKINE-HORNUNG, A., AND ŠŸKORA, D. 2013. Painting by feature: texture boundaries for example-based image creation. *ACM Transactions on Graphics (TOG)* 32, 4, 116.
- LUKÁČ, M., FIŠER, J., ASENTE, P., LU, J., SHECHTMAN, E., AND ŠŸKORA, D. 2015. Brushables: Example-based edge-aware directional texture painting. In *Computer Graphics Forum*, vol. 34, Wiley Online Library, 257–267.
- OLSZEWSKI, K., LIM, J. J., SAITO, S., AND LI, H. 2016. High-fidelity facial and speech animation for vr hmds. *ACM Transactions on Graphics (TOG)* 35, 6, 221.
- PATHAK, D., KRÄHENBÜHL, P., DONAHUE, J., DARRELL, T., AND EFROS, A. 2016. Context encoders: Feature learning by inpainting.
- PORTILLA, J., AND SIMONCELLI, E. P. 2000. A parametric texture model based on joint statistics of complex wavelet coefficients. *International journal of computer vision* 40, 1, 49–70.
- RITTER, L., LI, W., CURLESS, B., AGRAWALA, M., AND SALESIN, D. 2006. Painting with texture. In *Rendering Techniques*, 371–376.
- SELIM, A., ELGHARIB, M., AND DOYLE, L. 2016. Painting style transfer for head portraits using convolutional neural networks. *ACM Transactions on Graphics (TOG)* 35, 4, 129.
- SIDDIQUI, H., AND BOUMAN, C. A. 2008. Hierarchical color correction for camera cell phone images. *IEEE Transactions on Image Processing* 17, 11, 2138–2155.
- SIMONYAN, K., AND ZISSERMAN, A. 2014. Very deep convolutional networks for large-scale image recognition. *CoRR abs/1409.1556*.
- TSAI, Y.-H., SHEN, X., LIN, Z., SUNKAVALLI, K., AND YANG, M.-H. 2016. Sky is not the limit: Semantic-aware sky replacement. *ACM Transactions on Graphics (TOG)* 35, 4, 149.
- ULYANOV, D., LEBEDEV, V., VEDALDI, A., AND LEMPITSKY, V. 2016. Texture networks: Feed-forward synthesis of textures and stylized images. *arXiv preprint arXiv:1603.03417*.
- ULYANOV, D., VEDALDI, A., AND LEMPITSKY, V. 2016. Instance normalization: The missing ingredient for fast stylization. *arXiv preprint arXiv:1607.08022*.
- WEI, L.-Y., AND LEVOY, M. 2000. Fast texture synthesis using tree-structured vector quantization. In *Proceedings of the 27th annual conference on Computer graphics and interactive techniques*, ACM Press/Addison-Wesley Publishing Co., 479–488.
- WIKIPEDIA, 2017. Histogram matching — wikipedia, the free encyclopedia. https://en.wikipedia.org/w/index.php?title=Histogram_matching&oldid=723048018.
- YAN, Z., ZHANG, H., WANG, B., PARIS, S., AND YU, Y. 2016. Automatic photo adjustment using deep neural networks. *ACM Transactions on Graphics (TOG)* 35, 2, 11.
- YANG, C., LU, X., LIN, Z., SHECHTMAN, E., WANG, O., AND LI, H. 2016. High-resolution image inpainting using multi-scale neural patch synthesis. *arXiv preprint arXiv:1611.09969*.
- ZHU, J.-Y., KRÄHENBÜHL, P., SHECHTMAN, E., AND EFROS, A. A. 2016. Generative visual manipulation on the natural image manifold. In *European Conference on Computer Vision*, Springer, 597–613.